monotonically decreasing one. If a good thickness measurement can be performed near the beginning of the run, the subsequent thicknesses can be ascertained by examining the various results obtained from the order ambiguity and choosing the one which would best fit the known characteristics of the curve. Again the technique of calibrating on the bare substrate at the end of the measurement was used.

A typical graph of thickness versus time obtained using these techniques is shown in Fig. 6. The total time required for data acquisition is of course dependent on development rate and thus on exposure time and other related parameters. Data reduction again required approximately one to two seconds per point, with between 50 and 400 points generally used. Thus, in the worst case, 10 min is required for the data reduction. The previous techniques using numerous exposed resist samples and multiple development steps required weeks to complete a series of measurements and still resulted in far less accurate data than the present technique.

Thus a technique has been described which can be used for rapid *in-situ* monitoring of changing dielectric film thicknesses. Several practical examples of the use of this procedure have been given; they are meant to serve as typical applications. With some ingenuity and software modifications, this approach can be extended to other etching reactions as well as film growth processes.

REFERENCES

[1] K. L. Konnerth and F. H. Dill, "IOTA, a new computer controlled thin film thickness measurement tool," *Solid-State Electron.*, vol. 15, pp. 371–380, 1972.

Modeling Projection Printing of Positive Photoresists

FREDERICK H. DILL, SENIOR MEMBER, IEEE, ANDREW R. NEUREUTHER, MEMBER, IEEE, JAMES A. TUTTLE, AND EDWARD JOHN WALKER, MEMBER, IEEE

***Abstract*—The accompanying papers "Optical Lithography" and "Characterization of Positive Photoresist" introduce the concepts of modeling using destruction of the photoactive inhibitor compound to describe exposure and a surface-limited removal rate to describe development together with the optical exposure parameters *A*, *B*, and *C* and a rate relationship, *R*(*M*), which characterize the photoresist for modeling purposes. This paper applies the model to the projection exposure environment: exposure and development of photoresist are treated with a simulation model that allows computation of image surface profiles for positive photoresist exposed with a diffraction limited real image.**

INTRODUCTION

PROJECTION exposure of photoresist is of growing importance in the drive toward more complex microcircuits with smaller dimensions and fewer defects. It has found common usage in mask making and is beginning to be used for direct exposure of resist on silicon wafers. This paper applies the photoresist exposure and development model to the projection exposure environment, including experimental results supporting the model [1]. The concepts of A, B, C, and $R(M)$ and their determination, contained in the accompanying papers, are useful for any resist exposure technique provided that the optical environment is analyzed with adequate care.

The photoresist process model represents a powerful tool for studying projection exposure, because process control requirements for projection printing are extremely critical. With the model, the important parameters can easily be identified and a quantitative relationship established between them and the resultant image variations. By paying careful attention to the optics of image formation and photoresist exposure, we can use the A, B, and C parameters to calculate exposure distributions within the resist film as expressed by a relative inhibitor distribution, M, after exposure. Making use of the development rate curve, $R(M)$, the removal of the photoresist by the developer can be simulated and image surface profiles resulting from exposure and development can be calculated. These calculations are carried out for line-stripe patterns as commonly used in microelectronics structures.

PROJECTION PRINTING

Projection exposure of photoresist uses a lens to image a mask pattern onto the photoresist film. This represents one of the more challenging areas of classical optics, for

Manuscript received February 14, 1975; revised March 18, 1975.
F. H. Dill and E. J. Walker are with IBM Thomas J. Watson Research Center, Yorktown Heights, N. Y. 10598.
A. R. Neureuther is with the Department of Electrical Engineering and Computer Sciences, University of California, Berkeley, Calif. 94720.
J. A. Tuttle is with IBM, Route 52, Hopewell Junction, N. Y. 12533.

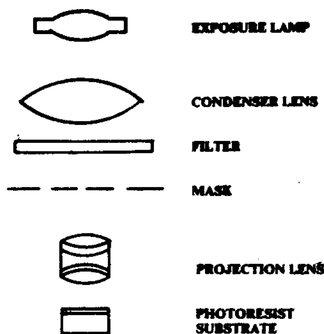

Fig. 1. Typical projection exposure environment.

one wants to maximize resolution of the image used to expose the photoresist while also meeting requirements for field size, depth of focus, field flatness, distortion, magnification control, and exposure wavelength. Remarkable progress has been made in exposure optics to allow exposure with micrometer size images over several millimeter fields or images of a few micrometers over full semiconductor wafers [2].

Fig. 1 schematically shows a typical projection exposure environment. The entire optical system is optimized for its intended purpose of highest possible resolution over a given field size. This means that the light source and its condenser come as close as possible to uniformly filling the entrance pupil of the projection lens. They are designed to provide uniform illumination over the entire mask object. The projection lens is designed for maximum resolution and is diffraction-limited—i.e., the resolution of the lens is determined by its aperture, not by imperfections of design or manufacture.

If we describe these optical systems as perfect, it is because they can be that way. Such systems can and have been built and produce images as predicted by their design. Not all projection systems are designed and made this well, but their optical performance can be measured and used in the model.

Because of design requirements, most optical projection systems are restricted to a narrow wavelength band usually corresponding to a single spectral line from the illumination source. In this paper, we consider monochromatic projection exposure only. Although the modeling extends readily to polychromatic exposure, we presently have too little experience with such systems to do meaningful simulations.

Any useful photoresist exposure is complex optically within the resist. In addition to the optical image forming process, we must deal with a strong optical absorption which bleaches as the photoresist is exposed and with coherent interference effects due to a reflecting substrate. Fortunately, we can separate variables well enough to attack the problem.

We assume that the incident illumination pattern (real image forming process) can be separated from the optical processes within the resist (exposure, absorption, and interference). The real image exposing the photoresist is treated as an intensity distribution incident on the photoresist surface. Within the resist, exposure distributions are calculated assuming that the exposing illumination has normal incidence and can be described at any point on the resist surface by an incident intensity value. This latter calculation includes the optical absorption and interference effects and computes exposure distributions within the film as a function of incident energy. It is useful for exposure environments other than projection printing, including resist exposure by a uniform incident light flux treated in the accompanying paper "Optical Lithography."

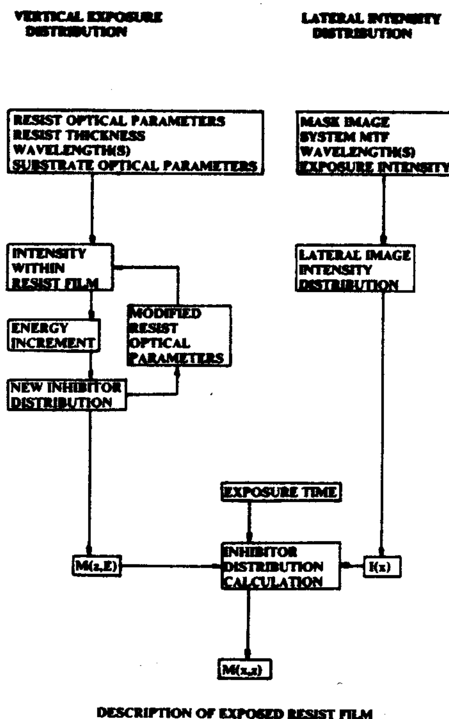

Fig. 2. Flow chart of inhibitor calculation for projection printing.

Thus the problem is separated into two parts: calculation of the image intensity distribution resulting from a known optical system, and calculation of exposure distributions within the resist for varying values of incident intensity and the given exposure time. The former is straightforward using Fourier optical theory; the latter can be done by extending thin-film optical computation techniques to handle the exposure dependent absorption of the photoresist.

The assumption of normal incidence for the exposure calculation is excellent for low numerical aperture ($NA < 0.2$) systems with limited resolution but is questionable for ultimate resolution systems ($NA > 1.0$) which can create resist images of a fraction of a micrometer. Most systems finding practical applications in microelectronics are closer to the lower limit with $NA = 0.15$ typical for full wafer exposure and $NA = 0.35$ typical for optics used to expose a single complex integrated circuit.

Fig. 2 charts the calculation of the inhibitor distribution for positive photoresist exposed in a projection environ-

ment. Inhibitor distribution, $M(x,z)$, our description of the chemical modification of the resist film by exposure, is relative to the photoactive inhibitor present before exposure. The concept of relative inhibitor concentration is treated in detail in the accompanying paper "Characterization of Positive Photoresist."

CALCULATION OF PHOTORESIST EXPOSURE FOR UNIFORM INCIDENT FLUX

The resist exposure calculation for projection printing is the same as a calculation of exposure level within the photoresist for a uniform incident flux, except that it must be carried out for the range of incident energies described by the image intensity profile and the exposure time. In order to do this calculation, we must have a complete understanding of the thin-film optical environment of which the photoresist is part.

Typically, we have a substrate surface such as silicon or a metal film which is opaque, smooth, and somewhat mirror-like. Overlying this may be thin transparent or semitransparent layers such as oxides, polycrystalline silicon, etc. These typically range from a few nanometers to several micrometers in thickness. On top of this, the photoresist is applied as a thin film, typically between 0.3 and 2 μm thick.

Anyone familiar with optical interference coatings would regard this as a complex optical environment that will have wavelength dependent properties. Reflections occur at each interface giving rise to optical interference effects within the photoresist. This is further complicated by the strong optical absorption of the photoresist which changes as it is exposed.

In a transmission line analogy, the substrate may be viewed as a termination and each dielectric layer as a transmission-line section with a characteristic impedance:

$$z = \frac{z_0}{\mathbf{n}} \tag{1}$$

where $\mathbf{n}$ is the complex index of refraction of the layer and z_0 is 377 Ω, the impedance of free space. The length of the transmission lines is typically on the order of the exposing wavelength, so that this series connection of unmatched lines will have significant electromagnetic standing waves present during exposure.

In order to do any calculations of resist exposure, we must know the optical constants of the substrate and any overlying layers. In addition, we must know the thickness of the overlying layers. At this time, we consider only specular (mirror-like) reflections with no scattering by the substrate or thin-film layers. These are reasonable assumptions for microelectronics except for resist applied over rough metallic films sometimes used for conductors. The modeling techniques have not yet been extended to include diffuse reflecting substrates.

The exposure parameters A, B, and C are the key to describing the exposure dependent optical properties of the photoresist. A and B, exposure dependent and independent parameters, describe the absorption constant α according to

$$\alpha = AM(z,t) + B \tag{2}$$

where M is the relative amount of photoactive inhibitor present at any position, z, and time, t, during exposure.

For optical computation purposes, we prefer to use the complex index of refraction of the photoresist

$$\mathbf{n} = n - ik \tag{3}$$

where n is the real part of the index ($n = 1.68$ for AZ1350J photoresist and a 404.7-nm wavelength) and k is the extinction coefficient

$$k = \frac{\alpha\lambda}{4\pi}; \qquad k \sim 0.02 \tag{4}$$

where λ is the exposing wavelength. Combining (2), (3), and (4) gives

$$\mathbf{n} = n - i\frac{\lambda[AM(z,t) + B]}{4\pi}. \tag{5}$$

The complex index of refraction changes as the inhibitor is destroyed by the exposing light with local intensity, I. The optical sensitivity parameter, C, relates the rate of destruction of inhibitor to the light intensity, as in

$$\frac{\partial M(z,t)}{\partial t} = -I(z,t)M(z,t)C. \tag{6}$$

The light intensity can vary greatly within the resist film over distances small compared to the resist film thickness due to interference between the incoming illumination and its reflection from the substrate. This results in a nonuniform inhibitor concentration and a corresponding nonuniformity in the complex index of refraction.

We use thin-film optical computation techniques to calculate the exposure distribution within the resist. Because the resist optical properties vary during exposure as a function of depth into the photoresist, we mathematically subdivide the resist film into sublayers thin enough to be treated as if they had isotropic properties. The interference effects have a periodicity of $\lambda/2n$ so that the sublayers must be thin compared to this. Sublayer thickness, δz_j, is usually chosen to be 5–10 nm while $\lambda/2n$ is typically 120 nm.

Berning [3] shows a convenient and consistent way to handle thin-film optical computations on a digital computer. He is able to calculate complex reflection (r_j) and transmission (t_j) terms for each interface referred to an air ambient ($n_0 = 1$), starting from the substrate. Fig. 3 diagrams the substrate and its overlying layers and the terms used in the computation. At the substrate $(m + 1)$

$$r_m = \frac{n_0 - \mathbf{n}_{m+1}}{n_0 + \mathbf{n}_{m+1}} \tag{7}$$

$$t_m = \frac{2(n_0 R[\mathbf{n}_{m+1}])^{1/2}}{n_0 + \mathbf{n}_{m+1}}. \tag{8}$$

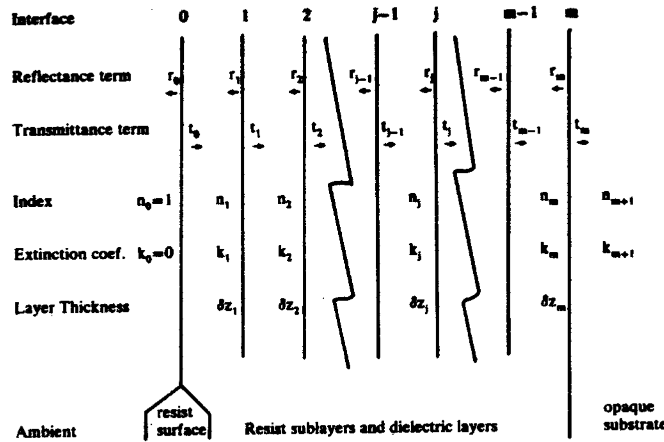

Fig. 3. Diagram of substrate and overlaying layers showing computational notation.

For the jth layer,

$$r_{j-1} = \frac{[\exp(-2i\phi_j)](F_j - r_j) - F_j(1 - F_j r_j)}{F_j[\exp(-2i\phi_j)](F_j - r_j) - (1 - F_j r_j)} \quad (9)$$

$$t_{j-1} = \frac{(F_j^2 - 1)t_j[\exp(-i\phi_j)]}{F_j[\exp(-2i\phi_j)](F_j - r_j) - (1 - F_j r_j)} \quad (10)$$

where

$$F_j = \frac{n_0 - n_j}{n_0 + n_j} \quad (11)$$

is the classical Fresnel coefficient referred to air and

$$\phi_j = \frac{2\pi}{\lambda} n_j \delta z_j \quad (12)$$

is the optical phase thickness of each layer.

Starting from the substrate interface $j = m$, we calculate r_j and t_j for each dielectric layer and resist sublayer until we reach the resist surface (r_0 and t_0). The reflectance and transmittance of the substrate coated with the dielectrics and resist are given by

$$R = |r_0|^2 \quad (13)$$

$$T = |t_0|^2. \quad (14)$$

We can calculate the absorbtance A_j of each resist sublayer from the ratio of the Poyntings vectors, P_j, at the interfaces for each layer, as seen by

$$\frac{P_j}{P_{j-1}} = \frac{|t_{j-1}|^2 (1 - |r_j|^2)}{|t_j|^2 (1 - |r_j - 1|^2)} \quad (15)$$

$$A_j = (1 - R)\left(1 - \frac{P_j}{P_{j-1}}\right) \prod_{1 \le q \le j-1} \left(\frac{P_q}{P_{q-1}}\right). \quad (16)$$

Here the computation starts at the surface ($j = 0$) and proceeds inward through the resist film.

The absorbtance can be used to calculate the average optical intensity, I_j, exposing the resist in the jth layer, as seen by

$$I_j = \frac{I_0 A_j}{(AM_j + B)\delta z_j}. \quad (17)$$

The rate of the destruction of inhibitor is proportional to the inhibitor concentration, the optical intensity, and the optical sensitivity parameter C, as given by

$$\frac{\partial M_j}{\partial t} = -I_j M_j C. \quad (18)$$

As the inhibitor is destroyed, the absorption coefficient of each layer changes. We treat this by dividing the computation into time (i.e., exposure) steps small enough that the changes in intensity within the resist are small, which is to say that the changes in inhibitor concentration are kept small. We proceed by calculating I_j holding the inhibitor concentration constant, incrementing the exposure time variable by Δt_e, and calculating new values of M_j so that the computation of I_j can be repeated. M_j is altered by exposure according to

$$M_j|_{t_e + \Delta t_e} = M_j|_{t_e} \exp(-I_j C \Delta t_e) \quad (19)$$

with the initial boundary condition that

$$M_j|_{t_e = 0} = 1. \quad (20)$$

The values of resist layer thickness δz_j and exposure increment Δt_e can be chosen by testing the convergence of the calculations. The computations converge to the correct theoretical value as δz_j and Δt_e are reduced to zero. The accuracy falls off as they are increased. Reasonable accuracy can be obtained if $\delta z_j < 0.03\lambda$ and Δt_e is chosen such that the largest change in any M_j is 0.2 or less.

These computations have been programmed in interactive APL [4] to allow flexibility in calculating M as a function of depth into the resist and exposure energy. Substrate, dielectric layers, resist thickness, and all associated parameters can be varied and exposure distributions

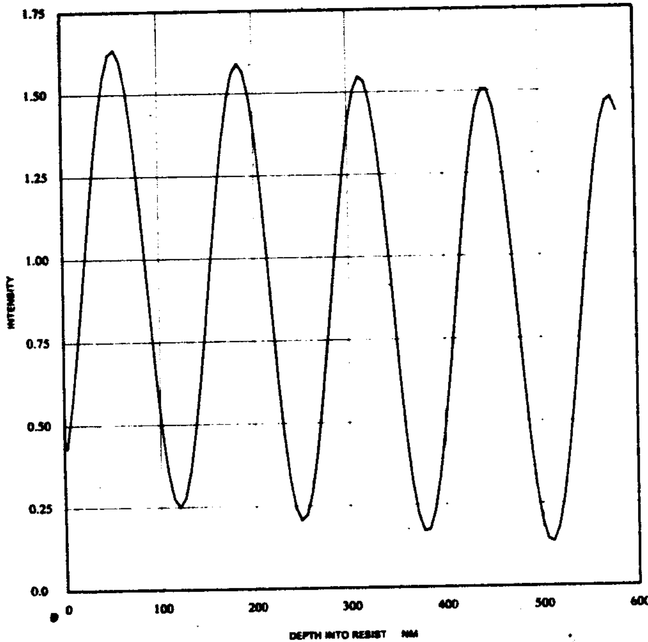

Fig. 4. Intensity of exposing light within a 584-nm AZ1350J photoresist film on 60 nm of oxide on silicon.

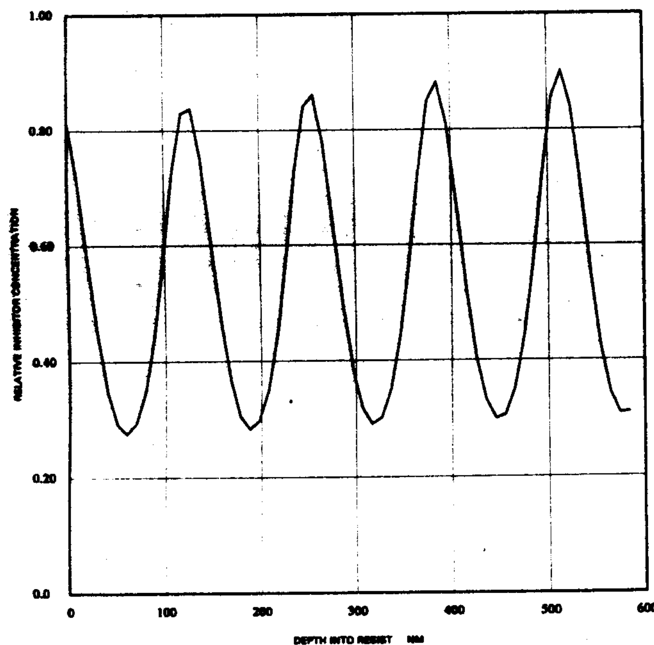

Fig. 5. Inhibitor concentration within a resist film on oxide on silicon after exposure to 57 mJ/cm² at a wavelength of 435.8 nm.

computed for a set of exposure energy increments up to some maximum value.

Fig. 4 shows a computation of the intensity distribution $I(z)$ within a 584-nm photoresist film on silicon with a 60-nm SiO_2 layer at the beginning of exposure by a uniform incident illumination at 435.8-nm wavelength. Fig. 5 shows the resultant inhibitor concentration after an exposure flux of 57 mJ/cm². This is typical of a "uniform" exposure of photoresist on a real substrate. Clearly both intensity and the exposure level as represented by the inhibitor concentration, $M(z)$, are very nonuniform, even in this very thin film of resist.

INTENSITY DISTRIBUTION OF A REAL IMAGE

The vertical coherence effects we see in the resist exposure of Fig. 5 have a spacing from intensity maximum to intensity minimum of $\lambda/4n$ or about 60 nm. The images used to expose photoresist seldom have spacings from maximum to minimum of less than 1000 nm. This allows us to separate the computations of vertical coherence effects from the intensity distribution incident on the resist film.

Most projection systems are designed to provide a diffraction-limited image over the entire image field. With a few exceptions, the systems are monochromatic, allowing the projection lens to be optimized for resolution, field flatness, and distortion without the additional complication of chromatic correction. We calculate intensity profiles for diffraction-limited lenses recognizing that, if the lens is less than perfect, it will not perform as well as described. If the performance factors of a less than perfect optical system are known, they can be introduced into the model with no difficulty. This can be done specifically to look at the effects of defocus for a perfect lens.

Modulation transfer function (MTF) techniques [5] represent a powerful tool for computing the image response of optical systems. The MTF of a diffraction limited optical system is given by

$$\mathrm{MTF}(\nu) = \frac{2}{\pi}\left[\cos^{-1}\frac{\nu}{\nu_0} - \frac{\nu}{\nu_0}\left\{1 - \left(\frac{\nu}{\nu_0}\right)^2\right\}^{1/2}\right] \quad (21)$$

where ν is the spatial frequency variable and ν_0 is the optical cutoff frequency of the system determined by its numerical aperture, NA, and the wavelength, λ:

$$\nu_0 = \frac{2\mathrm{NA}}{\lambda}. \quad (22)$$

Fig. 6 shows the MTF of a diffraction limited lens dropping from unity for zero spatial frequency to zero at the cutoff frequency, ν_0.

The object spatial frequency distribution, $I_0(\nu)$, is given by the Fourier transform, F_T, of the intensity description of the object, $I_0(x)$ as in

$$I_0(\nu) = F_T I_0(x). \quad (23)$$

In practice, we use a discrete Fourier transform with an implied periodicity. The image spatial frequency distribution, $I_i(\nu)$, is given by

$$I_i(\nu) = \mathrm{MTF}(\nu)[I_0(\nu)] \quad (24)$$

and the intensity description, $I_i(x)$, is given by the inverse (repeated) Fourier transform of the image spatial fre-

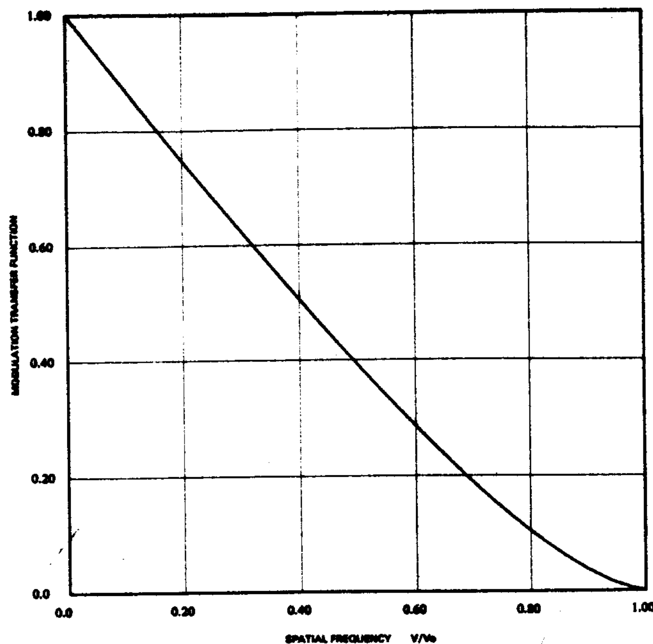

Fig. 6. Modulation transfer function for a diffraction limited lens.

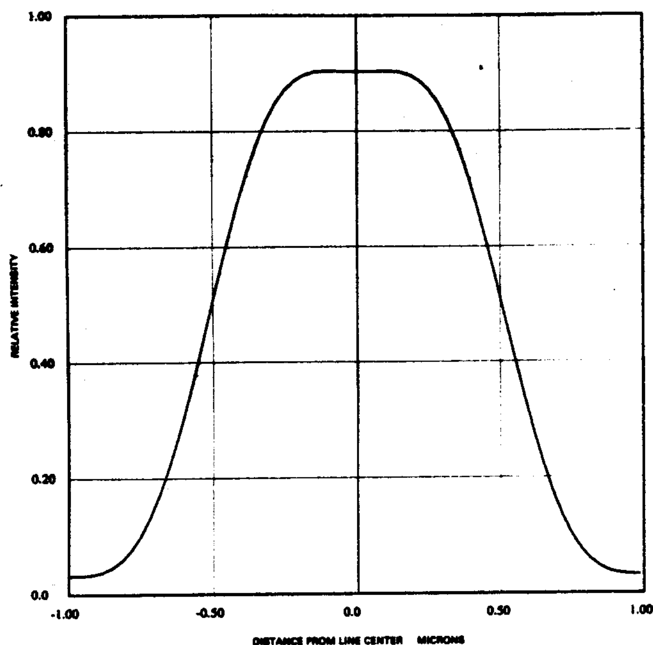

Fig. 7. Intensity distribution in the image of a 1-μ line imaged by a NA 0.45 lens at 435.8-nm wavelength.

quency distribution

$$I_i(x) = \mathrm{F_T}^{-1}[I_i(\nu)]. \tag{25}$$

Fig. 7 shows the calculated intensity distribution for the image of a nominal 1-μm line object produced by an NA 0.45 lens with a 435.8-nm wavelength.

This incident intensity distribution multiplied by the exposure time gives the incident energy distribution across the surface of the resist film. For computation purposes, $I_i(x)$ is calculated for discrete intervals across the surface

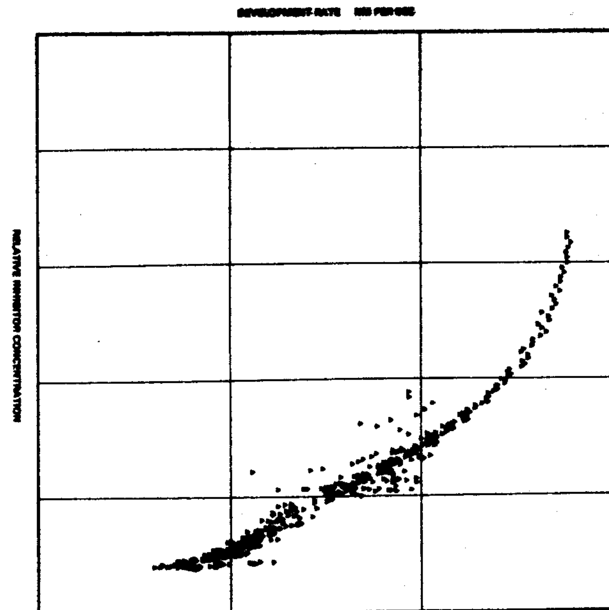

Fig. 8. Development rate for AZ1350J photoresist in 1:1 AZ developer: water at 20°C.

of width δx, over which the intensity incident on the resist can be considered constant.

By interpolation, we determine the $M(z)$ distribution under each lateral unit from the one-dimensional calculation of $M(z)$ as a function of exposure energy. The result is a two-dimensional description of the inhibitor distribution, $M(x,z)$, within the resist after exposure in which the unit cell is considered to have constant exposure and dimensions δz_j into the resist and δx laterally.

DEVELOPMENT OF IMAGES IN PHOTORESIST

The description of a line image exposure in photoresist is a two-dimensional matrix of inhibitor concentration values. Development is modeled as a surface limited etching reaction controlled by the local inhibitor concentration. Using the $R(M)$ curve such as that shown in Fig. 8, development rate values can be substituted for the inhibitor concentration values giving an $R(x,z)$ matrix description of the photoresist film for development.

A cellular approach is taken to the development of the resist film. Development proceeds along a surface in contact with the developer. Cells are removed by the developer according to their etch rate and the number of sides of the cell in contact with the developer. When a cell is removed, the new cells exposed are allowed to start etching. Any cells having an additional side exposed have their projected time of removal updated. This approach was chosen because it is computationally much simpler than directly following the moving boundary.

The time to remove a cell with only the top surface exposed is given by

$$t_r = \frac{\delta z}{R_{ij}} \tag{26}$$

TABLE I
PARAMETERS USED FOR EXPOSURE OF 1-μm LINE IMAGE IN PHOTORESIST

Substrate	Si
SiO_2	60 nm
Photoresist	AZ1350J
	Lot 30000J
Thickness	583.6 nm
Exposure Constants	$A = 0.54/\mu m$
	$B = 0.03/\mu m$
	$C = 0.014\ cm^2/mJ$
	$n = 1.68$
Exposure Wavelength	435.8 nm
Exposure Energy	57 mJ/cm^2
Development	1:1 Az developer: H_2O
	22°C
Development Rate	$E_1 = 5.27$
	$E_2 = 8.19$
	$E_3 = -12.5$

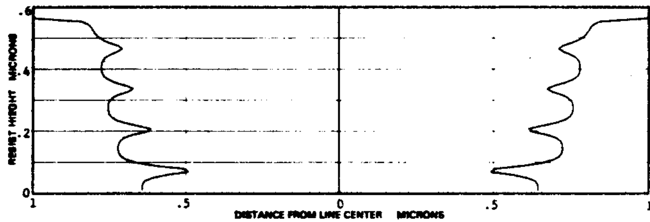

Fig. 9. Edge profile for a nominal 1-μ line in AZ1350 photoresist developed for 85 s in 1:1 AZ developer:water.

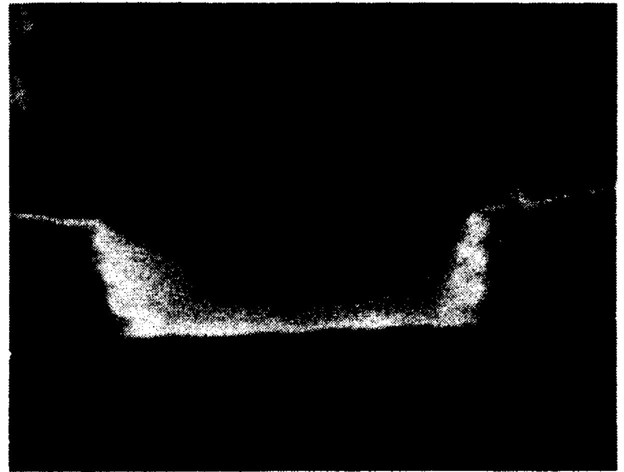

Fig. 10. Scanning electron micrograph of a 1.2-μ line in AZ1350J photoresist exposed with a nominal 1-μ image.

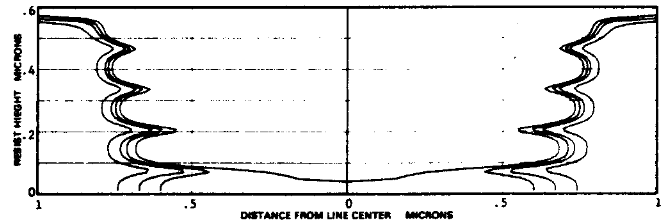

Fig. 11. Edge profiles for a nominal 1-μ line in AZ1350J resist developed for 70, 80, 90, and 120 s in 1:1 AZ developer:water.

where R_{ij} is the development rate associated with that particular cell and δz is the sublayer thickness. If top and one side are exposed,

$$t_r = \frac{\delta x \delta z}{R_{ij}(\delta x^2 + \delta z^2)^{1/2}} \tag{27}$$

where δx is the lateral dimension of the cell. Similar corrections are made for other combinations of cell faces exposed to the developer.

The APL program now in use calculates development starting at the top surface of the resist and proceeds until all the resist has developed away. It keeps track of the time at which each cell was removed so that contours of the resist image can be calculated for any development time.

Fig. 9 shows the edge profile of a nominal 1-μm line for a development time of 85 s; Table I shows the parameters associated with this example. The edge fringes on the line are typical for monochromatic projection exposure of AZ1350J. Fig. 10 shows a scanning electron microgram of a nominal 1-μm line exposed by projection through a NA 0.45 lens. The actual width of this line is 1.2 μm. The obvious line-edge fringes are totally invisible to optical microscopy because they are spaced closer than a half wavelength of visible light.

The agreement between observed linewidth and that calculated is not as good as for one-dimensional modeling. The NA 0.45 lens used in the experiments was not perfectly diffraction limited, and has a component of scattered light. Such a large numerical aperture makes the assumption of normal incidence for the exposing light less valid than for a smaller aperture; in addition, the experimental conditions for exposure and development are hard to completely characterize and control. Differences of up to 40 percent are seen in predicted linewidth for a given exposure and development, but general contour shape agreement has been good. More recent studies with systems with lower NA and improved experimental controls show much better agreement between experimental and calculated image profiles.

The modeling lends itself very easily to calculating the process sensitivities. Fig. 11 shows the same exposure as used in Fig. 9 with development times of 70, 80, 90, and 120 s. In Fig. 12, a curve of linewidth versus development time is shown. From this curve, it becomes clear that the process is less sensitive to variations in development if it is made larger than the nominal image size. This has been commonly recognized in many photoresist process areas where over-development is used to achieve good process control at the cost of pattern enlargement. Similar results can be obtained for variation of exposure time to establish process sensitivity to that parameter.

The monochromatic projection systems are particularly sensitive to thickness of photoresist and underlying dielectric layers. Odd multiples of a quarter-wavelength in total optical thickness of resist plus dielectric layers usually result in a minimum reflectivity at the resist surface and maximum energy coupling into the resist, whereas even quarter-wavelength multiples maximize reflectance and minimize energy absorbed in the resist.

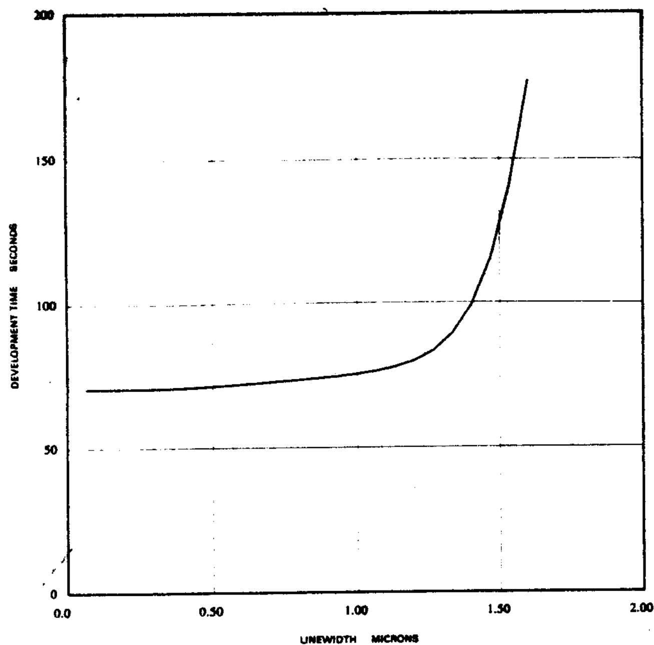

Fig. 12. Linewidth versus development time for a nominal 1-μ line in AZ1350J photoresist.

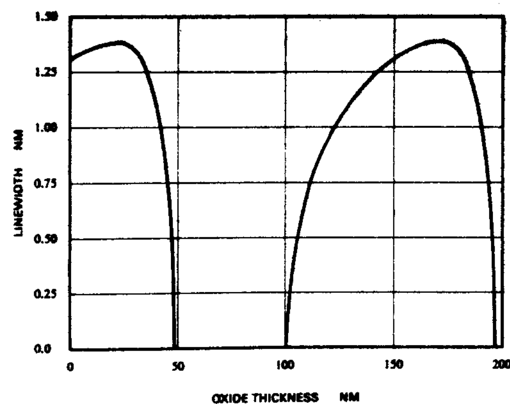

Fig. 13. Width of a nominal 1-μ line in photoresist as a function of underlying oxide thickness.

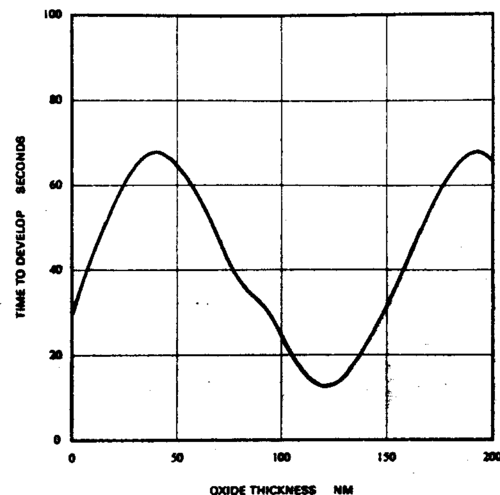

Fig. 14. Time to develop a 1-μ line in photoresist to nominal size as a function of underlying oxide thickness.

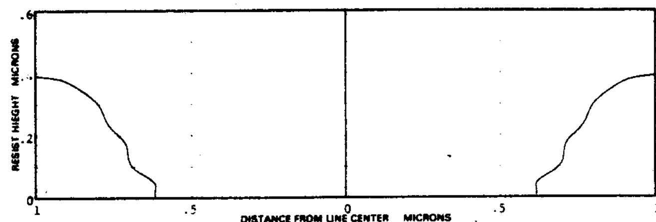

Fig. 15. Line-edge profile for AZ1350J resist developed in concentrated AZ developer.

This can result in changes in the exposure required to produce a given size line of up to a factor of two, which can mean the difference between creating the correct size opening with the resist image or having no opening at all.

Fig. 13 shows the variation of image size for a nominal 1-μm line as the oxide thickness under the resist is varied. Exposure and development are held constant. If we are trying to hold a 1-μm line size under these conditions, very tight control on oxide thickness is needed. A change of 10 nm in oxide thickness can change the resist image from one with the nominal 1-μm width to one with no opening at all.

Fig. 14 shows the process control expressed as the development time required to achieve the nominal 1-μm line as oxide thickness is varied. The variation is periodic in oxide thickness with a period of about 150 nm. A similar curve would apply to resist layer variation.

This critical sensitivity to layer thickness is due to the monochromatic illumination and the effect of film thicknesses on both standing wave ratio within the resist and reflection of light from the resist surface. The result seen here does not generalize to polychromatic illumination as is commonly used for contact printing. Resist exposure with polychromatic illumination will have a small dependence on the film thickness, particularly for thick resist films.

The development condition modeled here (1:1 AZ developer at 20°C), although commonly used, is a somewhat extreme example. The $R(M)$ curve shows a very low development rate (under 0.2 nm/s) for unexposed resist while reaching 100 nm/s for heavily exposed regions. With monochromatic exposure, most of the development time is spent removing the lightly exposed regions and little time with the heavily exposed ones. This high-contrast situation results in the relatively extreme fringing of the line edges, as seen in Figs. 9 and 10.

Concentrated AZ developer has a higher development rate for all M values, but, most significantly, for unexposed resist where the rate is about 3 nm/s. This results in a lowering of the rate difference between exposed and unexposed regions and it reduces the edge fringing. It does not eliminate the sensitivity of the line size to the resist and dielectric layer thicknesses since the exposure is still monochromatic. Fig. 15 shows a line edge simulated using the $R(M)$ curve for concentrated developer. The predicted line-edge shape agrees well with experimentally observed lines.

CONCLUSIONS

We have shown the application of the A, B, and C exposure parameters and the $R(M)$ development rate curve to modeling projection exposure and development of positive photoresist. The model correctly predicts fringes on image edges due to optical interference effects. It also clearly shows the need to carefully control layer thicknesses for a projection exposure process. The entire process can be studied and optimized to give the least sensitivity to critical parameters.

Image structures and parameter sensitivities are easy to study through modeling but are much more difficult to observe experimentally. For example, it is easy to vary resist thickness in 50-nm steps theoretically; achieving this experimentally is a difficult task. Without great care, experimental results have enough uncertainty to make quantitative measurement of process sensitivities impossible.

The use of the model for projection printing is only one example of its capability. It has been applied to creating integrated optics structures in photoresist [6]. It is presently being extended to cover other aspects of photolithography such as polychromatic exposure and thermal effects in resist processing. Other positive resist materials are being characterized so that their image forming properties can be compared to those already studied. The photoresist model can be applied equally well to the commonly used contact and near-contact printing methods, provided that the optical exposure environment is properly analyzed.

REFERENCES

[1] F. H. Dill, J. A. Tuttle, and A. R. Neureuther, "Modeling positive photoresists," Proc. Kodak Microelectronics Seminar, San Diego, Calif., Oct. 1974.

[2] R. E. Tibbets and J. S. Wilczynski, "High-performance reduction lenses for microelectroic circuit fabrication," *IBM J. Res. Develop.*, vol. 13, pp. 192–196, Mar. 1969.

[3] P. H. Berning, "Theory and calculations of optical thin films," in *Physics of Thin Films, Vol. I*, George Hass, Ed. New York: Academic Press, 1963, pp. 69–121.

[4] K. E. Iverson, *A Programming Language*. New York: Wiley, 1962.

[5] L. Levi, *Applied Optics, Vol. I*. New York: Wiley, 1968.

[6] A. R. Neureuther and F. H. Dill, "Photoresist modeling and device fabrication applications," Proc. Microwave Research Institute Symp. XVIII, New York, Apr. 1974.

Reduction of Photoresist Standing-Wave Effects by Post-Exposure Bake

EDWARD JOHN WALKER, MEMBER, IEEE

***Abstract*—A process is described for reducing the residual effects of standing waves upon exposed and developed lines in positive photoresist films.**

INTRODUCTION

WHEN photoresist films are exposed using monochromatic radiation, as in optical projection printing, standing waves are formed in the resist. The intensity in the resist varies periodically in the direction perpendicular to the plane of the resist, with a period $\lambda_r/2$ (typically 1300 Å). The intensity standing-wave ratio in this pattern can be as large as 9.

Another paper [1] examines experimentally the consequences of this situation for line-edge shape and linewidth control, and gives a simple physical model of the interference effects observed in resist films over a reflecting substrate. The purpose of the present paper is to describe a process for reducing the effect of standing waves on photoresist exposure and development.

Fig. 1(a) shows an SEM photograph of the cross section of a 1-μm wide line exposed in AZ-1350J photoresist in monochromatic illumination and developed by a conventional technique. The exposure was made at 4358 Å in a projection camera previously described in the literature [2]; the projection lens used was an 0.45-NA 25× Zeiss Epiplan. To produce the cross section, the wafer was cooled to liquid nitrogen temperature and fractured. The residual ridges on the wall of the developed line are a graphic indication of the locations of the minima in the standing wave pattern. The sample shown in Fig. 1(b) was developed in exactly the same manner as that in Fig. 1(a), except that the sample in Fig. 1(b) was baked for 10 min at 100°C after exposure, before development. The ridges apparent in Fig. 1(a) are markedly reduced in Fig. 1(b). It is to be emphasized that this effect is not connected with

Manuscript received January 2, 1975; revised March 3, 1975.
The author is at IBM Thomas J. Watson Research Center, Yorktown Heights, N. Y. 10598.